Macromol. Symp. **2008**, 262, 129–139 DOI: 10.1002/masy.200850213

Characterization of Highly Porous Materials from Cellulose Carbamate

Manfred Pinnow, Hans-Peter Fink, Carola Fanter, Jürgen Kunze*

Summary: Highly porous cellulose was formed by gelation of cellulose carbamate solutions in caustic soda. Two methods for gel preparation were optimized for the formation of beads and bulky materials – the chemical precipitation from dilute sulfuric acid and the thermal gelation by annealing at elevated temperatures. Various methods were used for characterizing of the pores of low density materials: scanning electron microscopy, small angle X-ray scattering, mercury intrusion and nitrogen sorption. These methods were optimized and used for characterizing the complete pore system from micro to macro pores. The effects of different preparation (cellulose carbamate concentration in caustic soda) and processing (precipitation, drying and pyrolysis) on the pore structure were studied by the set of complementary methods. Aerocell samples with a minimum density of 0.06 g/cm^3 were prepared from cellulose carbamate. They are characterized by a broad pore size distribution ranging from 0.5 nm to 1 mm, specific internal surfaces of up to 660 m^2/g and total pore volumes of up to 18 cm^3/g.

Keywords: aerogels; cellulose carbamate; Hg-intrusion; N_2-sorption; pore structure; SAXS; SEM

Introduction

Aerogels are highly porous low density materials obtained by fixation of the wet gel state in the process of drying, as it was established for the formation of silica and also cellulose based aerogels by *S. Kistler*[1,2] in the 1930s. Within the 6th Framework Program of the European Union the Aerocell Project dealt with the preparation of cellulose based aerogel materials by novel routes. Besides the direct dissolution of cellulose in N-methylmorpholine-N-oxide (NMMO) monohydrate[3] and in aqueous NaOH-solution,[4] cellulose carbamate was used for the preparation of highly porous samples. Cellulose carbamate (CC) was synthesized in a heterogeneous reaction of cellulose and urea. CC is easily soluble in aqueous NaOH and can be used as a spinning solution[5] avoiding environmental hazards, e.g. C_2S emission in the viscose route. This paper focuses on the preparation and characterization of highly porous materials according to the cellulose carbamate route including the preparation of CC-solutions, the subsequent precipitation of CC, and the chemical or thermal decomposition. Also, effects of drying and pyrolysis were investigated. The pore structure of the materials in different stages was characterized by scanning electron microscopy, small-angle X-ray scattering, Hg-intrusion, and N_2-sorption methods.

Experimental Part

Aerogel Preparation:

Preparation of the CC-solution

Cellulose carbamate can be prepared by various synthesis routes.[5–7] In the present work cellulose carbamate was prepared using a kneader technique.[5] A softwood

---

Fraunhofer-Institute for Applied Polymer Research IAP, Geiselbergstr. 69, 14476 Potsdam-Golm, Germany
E-mail: manfred.pinnow@iap.fraunhofer.de

prehydrolysis kraft (PHK) pulp with a degree of polymerization (DPcuox) of 490 was activated by caustic soda and subsequently kneaded with an excess of urea at 130 °C. Finally, the CC was thoroughly washed and dried and thus conserved for further processing. The obtained CC was characterized by a DPcuox of 350 and a nitrogen content of about 2.76%, corresponding to a degree of substitution of $DS = 0.36$.

The cellulose gel was prepared from solutions with a CC-content from 1 to 8% in caustic soda. An aqueous solution of 7.3% w/w sodium hydroxide was cooled to −3 °C prior to adding dry CC to the caustic soda while the temperature was maintained. After a period of about 1.5 h a transparent solution was obtained, indicating that the CC was completely dissolved.

Solutions with CC contents of 3% and 5% turned out to be the most promising for the desired material properties. At the CC concentration of 1% the mechanical stability of the resulting cellulose gel decreased considerably so that the formation of stable samples was nearly impossible. At a higher CC concentration than 8%, the porosity decreased and too high densities of the materials were obtained.

Precipitation and Decomposition

Two different methods were used in order to precipitate the gels from the CC-solutions.

(i) Thermal precipitation was used to get bulky samples. Cylindrical samples with 40 mm in diameter and in height, respectively, were formed by filling the solutions into cylindrical glasses. The solution was heated to 105 °C and kept at this temperature for 2 h. In this procedure the CC was simultaneously precipitated and decomposed to alkali-cellulose, which was regenerated to cellulose by neutralization. Under release of ammonia gas, a cylindrical cellulose gel sample was formed.
(ii) Chemical precipitation was carried out in a cylindrical glass by covering the CC-solution carefully with 10% sulfuric acid having a well-defined salt content (e.g. 15% sodium sulfate) and the CC-gel was obtained. Finally, the CC was decomposed in aqueous caustic soda (7.3% w/w) at room temperature. Both subsequent steps, the penetration of the acidic precipitation solution and of the caustic decomposition solution into the cylindrical gel samples are diffusion-controlled processes and hence, comparatively time consuming. The formation of the gel body is complete after approx. 8 h.

The chemical precipitation is therefore more suitable for preparing of smaller samples, such as beads or fibers of a diameter of about 0.5 mm. Hence, beads having a diameter of 0.5 mm were formed by a jet-cutting procedure[8] which was developed by geniaLab GmbH (Braunschweig, Germany). Here, a jet of the CC-solution is cut by a rotating wheel and the droplets fall into the precipitation bath. Subsequently, the cellulose was regenerated as described above.

Finally, elemental analysis of dried samples revealed that neither after chemical nor after thermal precipitation and decomposition the corresponding samples contain any nitrogen. This indicated that the carbamate groups were completely removed and the resulting material was pure regenerated cellulose.

Washing, Exchange of Water and Drying

After regenerating the cellulose, water-soluble contents such as salts and base must be completely removed by washing with water - which is also a diffusion-controlled process. The washing of the beads is more effective, when a continuous flow of the beads is provided by stirring.

The wet aerocell samples were dried by applying two methods

- freeze drying (FD) after rapid freezing of the aerocell samples in liquid nitrogen,
- super critical drying (SCD) in carbon dioxide flow.

SCD was carried out by Natex GmbH[9] - after replacing the water inside the samples by an appropriate liquid medium, such as acetone or ethanol. The water was exchanged by increasing the acetone or ethanol content of the liquid phase surrounding the aerocell sample. To prevent the cellulose pore structure from collapsing, the content of acetone (resp. ethanol) was increased stepwise by 20% (v/v). Each step took a period of 24 h. The last step at 100% acetone (ethanol) had being repeated to ensure the complete exchange of water.

Pyrolysis

Selected samples were pyrolysed in order to get electrical conducting electrode material.[10] Pyrolysis was carried out at 800 °C for 5 h in a nitrogen flow by the project partner CEP (Centre Energetique et Procedes, Ecole des Mines, Sophia-Antipolis, France). The mass loss during pyrolysis was 89% - 93%, a cubic aerocell sample with an original side length of 5 mm shrank to about 1 mm^3 after pyrolysis.

Pore Characterization:

The specific properties of aerocell samples desired for the different applications strongly depend on certain well defined pore characteristics. Therefore, the pore size distribution, the specific pore volume, the corresponding bulk density and the specific pore surface were determined. It has been found that pore diameters cover the wide range from 500 μm to smaller than 0.5 nm. According to the IUPAC definition pores are classified into three groups: macro pores (>50 nm), meso pores (50 - 2 nm) and micro pores (<2 nm). The large range of pore diameters requires multiple, complementary methods to characterize the whole variety of pores which is necessary for elucidating structure-property relations and to get an idea of the influence of different parameters of preparation or processing on the structure and properties of the aerocell samples. To this end we used Hg-intrusion, N_2-sorption, small angle X-ray scattering (SAXS) and scanning electron microscopy (SEM). Each method was adapted to the specific subject. The methods and the corresponding range of pores are compared in Figure 1.

Scanning Electron Microscopy (SEM)

SEM was used to study the morphology and pore structures of the aerocell samples. The SEM images were taken by a JSEM 6330F (Jeol, Japan) at an acceleration voltage of 5 kV. Cross sections were prepared by fracturing the aerocell samples in liquid nitrogen and finally, a thin Platinum layer (thickness 4 nm) was sputtered on top of the cross section to avoid electrical charging by the electron beam. Both open and closed macro pores as well as also meso pores down to a diameter of 10 nm can be visualized by this method. Micro pores could not be detected because of the limited SEM resolution.

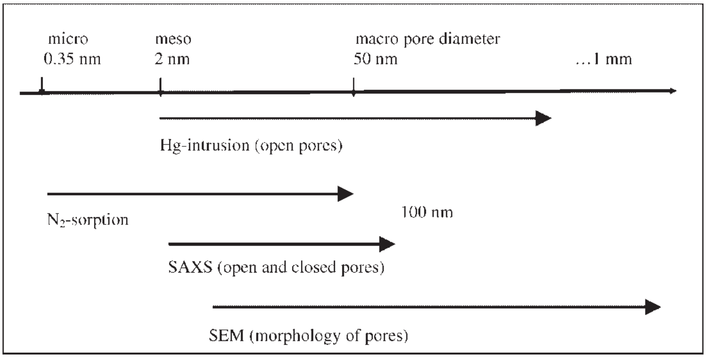

Figure 1.
Operating range of all methods used for pore size characterization.

The implement SEM equipment includes a tool for cryo-preparation, which allows to study the gel state in different stages of the preparation process (precipitation, decomposition). Other than with an environmental SEM,[11] for this purpose a droplet or a small sample with a diameter of up to 2 mm is rapidly be frozen in nitrogen slush. After fracturing the frozen sample, a definite amount of water is sublimated from the surface of the cross section which is finally Pt-sputtered before taking the SEM image at −160 °C.

Mercury Intrusion

Generally, mercury intrusion is a suitable method for characterizing open (accessible) macro and meso pores. This method was primarily used to determine the specific volume and the specific surface of the pores and to calculate the porosity and bulk density of the aerocell samples. Hg-intrusion was carried out combining the macro and meso pore units ‘‘Pascal 140’’ and ‘‘Pascal 440’’ (Porotec GmbH, Germany), respectively, and merging the data of both units in one distribution. To ensure the reproducibility of measurements, prior to Hg-intrusion the samples with a maximum volume of 2 cm^3 space were thoroughly dried and conditioned for 1 h in the recipient of the equipment (pressure 10 Pa) to remove moisture from the cellulose completely (hydrophilic cellulose adsorbs about 6% w/w water at normal conditions in room atmosphere).

The parameters of the pore size distribution were calculated from the curve of the cumulative pore volume, where the pore radius is related to the pressure applied on mercury by *Washborn's* equation[12] assuming cylindrical pore geometry. Generally, macro pores contribute mainly to the specific volume and therefore to the density of the aerocell samples, while meso pores contribute primarily to the specific pore surface.

Nitrogen Sorption

The distribution of meso and micro pores were studied by nitrogen-physisorption experiments using a ‘‘Sorptomate 1990’’ (Porotec GmbH, Germany). Prior to the measurements, all aerocell samples had to be preconditioned in order to ‘‘clean’’ the pore surface thoroughly from adsorbed species ($p = 10^{-2}$ Pa, $T = +90\,°C$, $t = 16$ h). The pore parameters were calculated from the fit of different models to the adsorption and desorption isotherms in the respective pressure region. The various models are based on different physical principles of physisorption. The approaches applied to the aerocell-isotherms are:

- BET: principle of monolayer adsorption; supplies the specific surface of meso pores,[13]
- BJH: principle of capillary condensation (*Kelvin* equation); supplies the size distribution of meso pores,[14]
- HK: starting from the *Lennard-Jones* potential, the HK-model supplies the size distribution of micro pores.[15]

Small Angle X-ray Scattering (SAXS)

Small angle X-ray scattering (SAXS) is a complementary method to study pores with colloidal dimensions (2–100 nm), and has been successfully applied for determining cellulose pore structures.[16] Other than the mercury intrusion, the SAXS method indicates also closed pores, i.e. the whole pore structure including closed and open macro and meso pores. The scattering effect being used in SAXS is caused by different electron densities of the studied phases. Supposing a two phase structure (cellulose pores) with sharp phase boundaries, the mean pore dimension (intersection length l_v/nm), the pore volume fraction (w_v/% v/v), and the specific inner pore surface ($S_{sp}/m^2/cm^3$) can be derived from the measured and corrected SAXS curve, according to the *Porod* theory.[17] Ni-filtered Cu-K_α radiation and a *Kratky* compact camera with a slit-like primary beam were used for the scattering experiments.

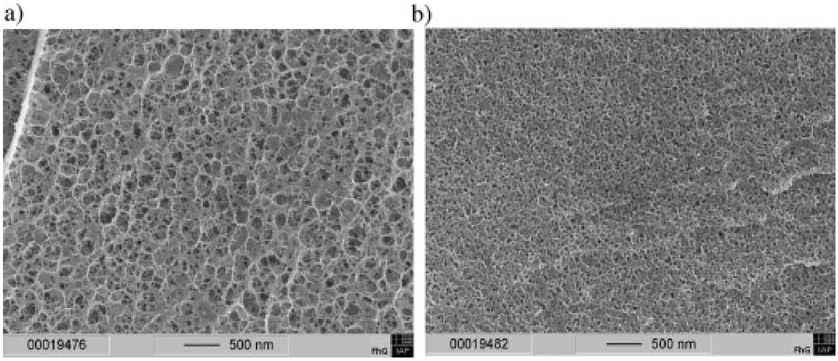

Figure 2.
SEM micrographs of never dried CC-gel droplets obtained by cryo-preparation from an 8% w/w CC-solution after chemical precipitation in sulfuric acid (2a) and subsequent chemical decomposition in caustic soda (2b).

Results and Discussion

Gel State

The formation of the pore structure in the CC-gel state was studied by SEM using a cryo-transfer technique as described above. A comparison of two corresponding SEM micrographs (Figure 2) reveals that the gel state after chemical precipitation is not stable and is affected by the subsequent decomposition process.

Figure 2a shows that after precipitation a gel is obtained which is characterized by a thickness of the pore walls of about 10 nm and a mean pore size of approx. 31 nm. After chemical decomposition of the CC, however, the pore diameter decreased to about 20 nm, whereas the density of the aerocell gel increased (Figure 2b). At the same time, the large pores with diameters of 100–200 nm disappeared.

Dry State

Drying of materials obtained from solution can be very challenging especially if certain structural features shall be preserved. As compared to the simple air-drying at elevated temperatures, freeze drying (FD) should preserve the pore structure of the initially wet cellulose to a higher degree.

SEM micrographs of the cross section of a sample after freeze drying are shown in Figure 3. After chemical precipitation, decomposition, and thorough washing with water, the large cylindrical samples were frozen in liquid nitrogen and freeze-dried

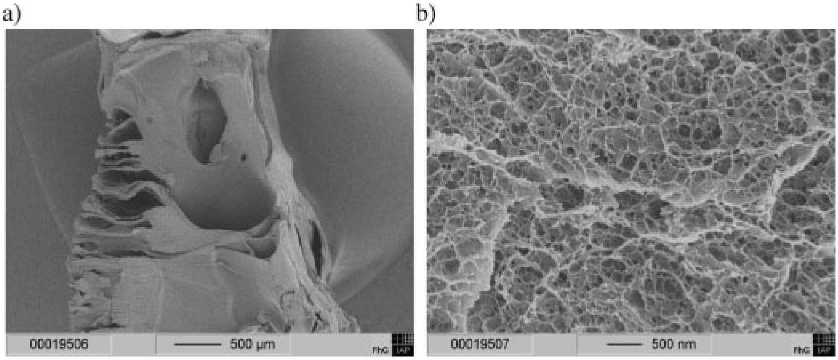

Figure 3.
SEM micrographs of freeze-dried samples with cracks (3a) and their pore system at higher magnification (3b). The cross sections were prepared by cryo-fracturing of the dried samples in liquid nitrogen.

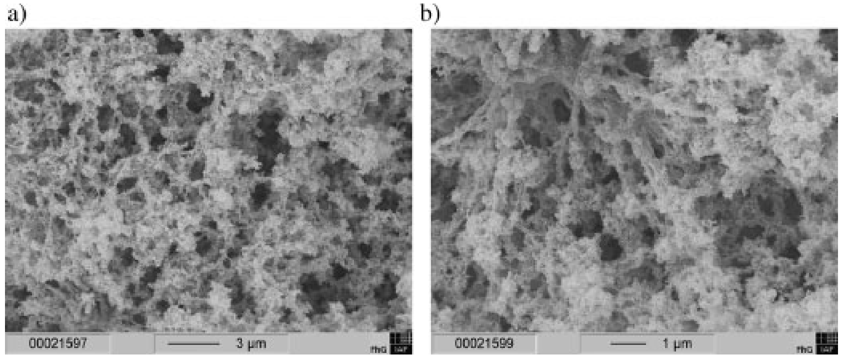

Figure 4.
SEM micrographs of the cross sections prepared by cryo-fracturing in liquid nitrogen with increasing magnification (a and b). The sample was dried super critically after water exchange by acetone.

for 24 h at −60 °C in vacuo. As Figure 3a shows, large cracks occurred as a result of the mechanical stress caused by the ice front moving through the sample during fast freezing of water in liquid nitrogen. Compared to the pore structure after the cryo-transfer preparation of small gel droplets (Figure 2) the macro and meso pores are enlarged and slightly deformed (Figure 3b). Nevertheless, the original structure of the pores in the gel state – filigree cellulose walls forming the pores – was preserved throughout FD.

A striking variation of the pore structure was observed by SEM after super critical drying (SCD). In both cases, after water exchange by ethanol and, more pronounced by acetone, the cellulose walls (Figure 3) did not appear or were hidden behind a dense web of fine fibers with a thickness of 10–20 nm (Figure 4). Based on appropriate evaluation of the N_2-sorption data, the effect of drying will be discussed more in detail.

However, at a first glance freeze-drying seems to be advantageous, as the time consuming process of water exchange is avoided and lower material densities of about 0.06 g/cm^3 are obtained, owing to a high amount of macro pores. On the other hand, voids and cracks (Figure 3a) in these aerocell samples can cause bursting of the

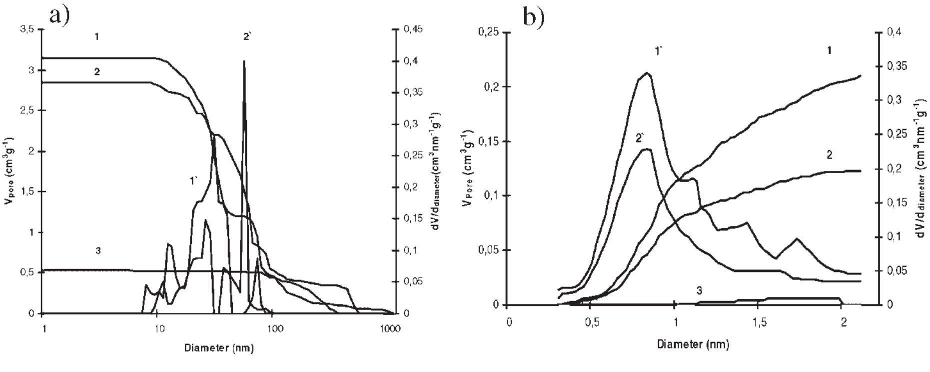

Figure 5.
Effect of drying on the distribution of meso pores (5a) and micro pores (5b) calculated from the BJH- and the HK-model, respectively: curves i – pore volume (left axis, [cm^3/g]), curves i′ – pore distributions (right axis, [cm^3/nm*g]) as functions of the pore diameter. The samples were prepared from a 3% CC-solution by thermal precipitation and subsequently freeze-dried (3) or super critically dried from acetone (2) or ethanol (1).

cellulose body during the freezing procedure which would reduce the mechanical stability. Furthermore, N_2-sorption experiments showed a complete collapse of the meso and micro pore structure after FD (Figure 5a and 5b).

Both Figures show no contribution of meso pores smaller than 20 nm and no contribution of micro pores to the cumulative pore volume after freeze-drying. The meso pore volume after FD amounts to 0.6 cm^3/g compared to about 3 cm^3/g after SCD. Further, SCD of ethanolic gel results in a slightly increased volume of meso and micro pores (3.1 and 0.25 cm^3/g) compared to SCD in acetone (2.8 and 0.14 cm^3/g). Hence, it can be concluded that most of small meso pores and the micro pores disappear in the course of the freeze-drying process. It seems that these pores are compressed or disrupt most likely caused by ice crystals growing outside or inside the water filled pores, respectively. Super critical drying of aerocell samples from ethanol has a slight advantage over SCD from acetone with respect to the preservation of the meso and micro pore system.

The results of mercury intrusion and nitrogen sorption of different aerocell samples are summarized in Table 1. The data reveal that the cumulative pore volume determined by Hg-intrusion was generally higher for the thermally precipitated samples than for the chemically precipitated ones. This result, which is mainly caused by the effect of macropores, could not be confirmed by the N_2-sorption values which are mainly affected by meso and micro pores. From N_2-adsorption it can be concluded that a lower polymer concentration in solution (3%) results in a higher cumulative volume and specific surface of the meso and micro pores. Thus, the macro pore structure is influenced by the precipitation route, whereas the micro and meso pore structure is predominately controlled by the polymer concentration in the starting solution.

Results of the SAXS method cannot be compared directly with those of the Hg and N_2 methods because SAXS reflects both open and closed pores. With SAXS we found typical values of 10 nm for the pore diameter and 580 m^2/g for the specific pore surface. Generally, the pore diameters from SAXS calculated as mean values for micro pores and small meso pores correspond roughly to the BJH and HK results (Figure 5) in this region. However, the SAXS data of the specific pore surface including the contribution of closed pores exceeded the data from N_2-sorption experiments significantly.

Pyrolysis

Further morphological changes were observed after pyrolysis of the aerocell samples (Figure 6). Here, we found distinct

Table 1.
Results obtained from mercury intrusion and nitrogen sorption experiments. The aerocell samples were prepared from a 3 or 5% CC–solution, precipitated thermally (th) or chemically (ch), dried super critically from acetone and pyrolized at 800 °C.

Sample preparation		Hg-intrusion					N_2-adsorption	
CC-solution		CV cm^3/g	SS m^2/g	$D_{macro}/\mu m$ (l/s)	P %	BD g/cm^3	CV $_{BJH}$ cm^3/g	SS $_{BET}$ m^2/g
3%/th.	before pyro-lysis	14.6	127	22/0.08	92	0.06	2.59	433
3%/ch.		6.2	53	25/0.08	–	0.06	2.66	429
5%/th.		11.9	197	15/0.16	92	0.08	1.96	382
5%/ch.		3.8	174	36/0.03	81	0.22	2.23	361
3%/th.	after pyro- lysis	3.6	210	21/0.03	87	0.24	0.77	567
3%/ch.		3.4	252	26/0.02	93	0.27	0.72	661
5%/th.		3.8	318	27/0.02	89	0.23	0.9	598
5%/ch.		4.0	237	27/0.03	84	0.21	0.92	492

CV - cumulative pore volume, SS - specific pore surface, D - diameter of the macro pores at the maximum of pore distribution (l/s – two peaks of large and small macro pores diameters), P – porosity, BD - bulk density of the samples.

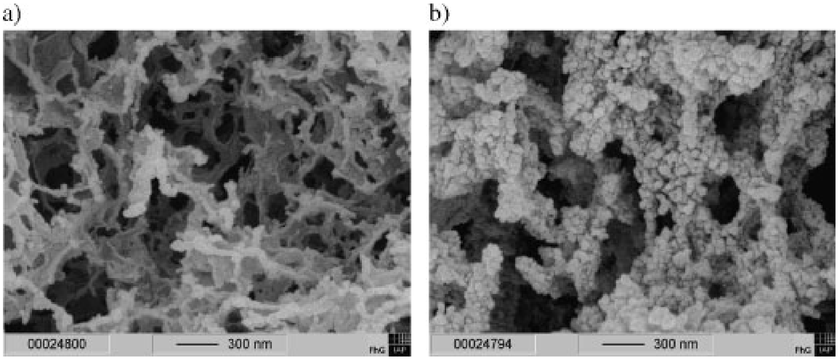

Figure 6.
SEM micrographs of pyrolized samples which were prepared by freeze-drying (6a) and super critical drying (6b). The cross sections were prepared by cryo-fracturing in liquid nitrogen.

differences between freeze-dried and super critically dried samples. In spite of the high mass reduction which was observed during the course of pyrolysis (typically 89–92% w/w) the wall-like structure of the FD samples and also the structure of the macro and meso pores were largely preserved. In SCD samples, however, carbon nano particles with a diameter of about 20–100 nm were formed and the fibrillar structure (Figure 4) disappeared completely. Figure 6 shows that the structure of the pyrolized aerocell samples is much denser and that the filigree cellulose walls and fibers disappeared while nano particles are formed.

The data in Table 1 indicate that the cumulative pore volume determined by Hg-intrusion before pyrolysis was higher for thermally precipitated samples than for chemically precipitated ones. After pyrolysis, the cumulative pore volume of the thermally precipitated samples was reduced and no significant difference to the chemically precipitated samples was observed. In addition, the specific pore surface of all samples increased through pyrolysis. Obviously, the amount of large macro pores (diameter 15–36 μm) was reduced in the course of pyrolysis and an additional maximum of smaller macro pores was emerged (compare Table 1, D_{macro}(s)). Considering that the pore specific surface increased after pyrolysis, we assume that large macro pores shrank and formed smaller pores. This is in accordance with the observed decrease in porosity and increase in the density of the pyrolysed aerocell samples, both effects being mainly caused by a reduced amount of large macro pores. Though the cumulative volume decreased, the observed increase of the specific surface can be due to a higher number of small pores.

Exemplary the results of the mercury intrusion experiments before and after the pyrolysis of a freeze-dried aerocell samples are provided in Figure 7. Both pore size distributions show a distinct amount of macro pores in the diameter range of 10–100 μm and hence, the cumulative pore volume decreased considerably after pyrolysis. In the same procedure additional species of meso pores with a diameter of about 15–20 nm emerged in freeze-dried samples (Figure 7b) analogous to SCD samples (Table 1, s – small pores). Taking into consideration the enormous shrinkage of the samples during pyrolysis, we conclude that the small pores are formed from larger pores by shrinking.

N_2-sorption experiments, predominantly in the region of meso pores, confirmed the above mentioned effect of pyrolysis: the cumulative volume decreased while the specific surface of meso pores increased, as was calculated form the BJH- and the BET-model (Table 1), respectively. Furthermore, the contribution of meso pores to the total specific surface is considerably higher than that of macro pores before and

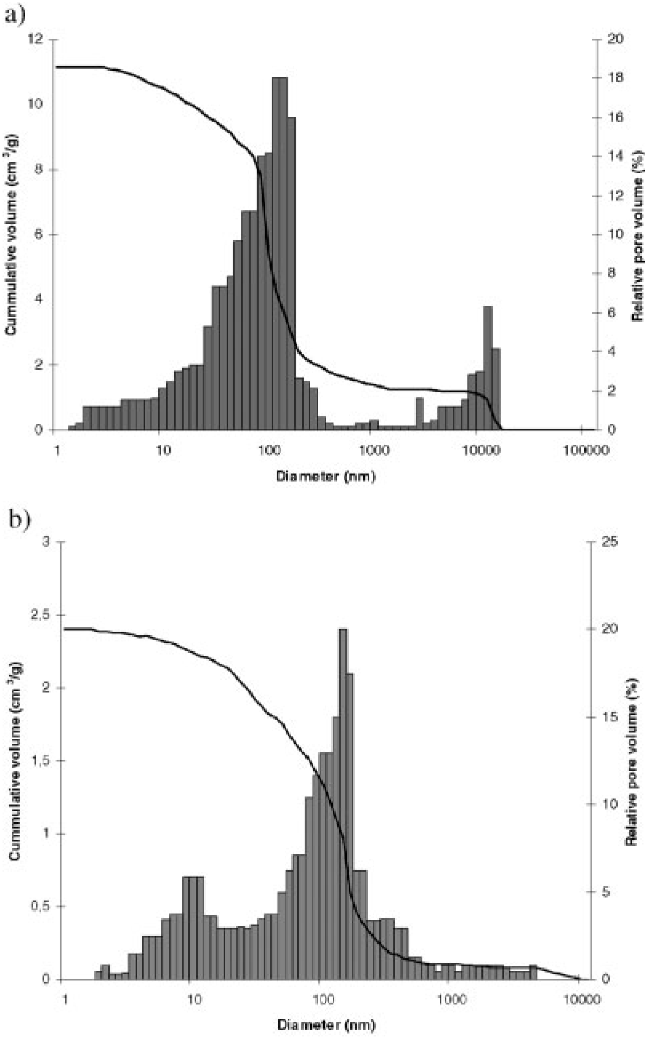

Figure 7.

Pore distributions of aerocell samples before (7a) and after pyrolysis (7b), obtained by mercury intrusion; cumulative pore volume (line, left axis in cm^3/g) and relative pore volume (bars, right axis in %) as functions of the pore diameter, which was calculated from the *Washborn's* equation assuming cylindrical pores.

after pyrolysis. Other than for macro pores, no significant differences in the cumulative volume and the specific surface were observed between thermally and chemically precipitated samples. The specific surface, however, increased after precipitation from CC-solutions with lower polymer concentration.

The results from SAXS-investigations clearly indicate that the diameter of meso pores (from 10 nm to 2.5 nm) as well as their volume fraction (from 30% to 7%) decreases in the course of pyrolysis. This result corresponds to the reduced cumulative volume of meso pores observed by N_2-sorption experiments for pyrolized samples. Taking into account the density of the pyrolysed samples of about 0.2 g/cm^3, a mass specific surface of 575 m^2/g was calculated from the volume specific surface of 115 m^2/cm^3 determined by SAXS. This value confirms the results from the N_2-sorption (Table 1). The high values for the specific surface from SAXS measurements were determined from the aerocell sample already before pyrolysis, indicating the existence of closed pores, which are not accessible for nitrogen before pyrolysis.

Conclusion

Highly porous cellulose materials can be obtained from cellulose carbamate solutions in caustic soda via chemical and thermal gelation. It has been found that the drying procedure is a very important step in order to preserve the highly porous gel structure. Complementary methods such as scanning electron microscopy, mercury intrusion, nitrogen sorption, and small-angle X-ray scattering were used to characterize the highly porous cellulose samples. The potentials and limitations of these methods were demonstrated.

Scanning electron microscopy was used for a first screening of the pore structure of aerocellulose samples in the gel state and after drying. The morphology of macro and meso pores down to a diameter of 10 nm was determined by this method and the SEM reflects the effects of various preparation parameters on the pore morphology. Although the pore structure could not quantified by means of the SEM pictures, qualitative features of the pore morphology are in good correlation with results from mercury intrusion regarding the porosity and the material density. Smaller meso pores and micro pores were not detected by the SEM method because of the limited contrast and resolution. We suppose that these pores are located inside the thin cellulose walls which form the macro and meso pores.

Quantitative characterization of the pore structure was realized by combining the results of mercury intrusion, nitrogen sorption and SAXS experiments. The methods complement one another, and by the combination of all these methods, parameters of the whole pore structure of the aerocell samples from macro pore to micro pore sizes are obtained. The effects of different preparation and processing parameters of aerocellulose including drying and pyrolysis were studied by these methods. It was shown that the preparation of the gel state from cellulose carbamate is a promising route to produce highly porous cellulose materials with a low density of up to 0.06 cm^3/g and a highly specific pore surface of about 430 m^2/g caused by the formation of a system of macro pores, meso pores and micro pores.

Acknowledgements: This work was carried out within the EC 6th framework program, project acronym AeroCell, contract number NMP3-CT2003-505888. The authors would like to thank all partners for broad discussions and fruitful cooperation. We would like to express our special thanks to S. Siebenhaar and U. Jahnz at geniaLab GmbH, who prepared the aerocellulose beads by a JetCutter, to E. Lack and M. Sova, who carried out the super critical drying at Natex GmbH and to S. Berthon-Fabry and A. Rigacci, who pyrolysed the aerocell samples.

[1] S. S. Kistler, *Nature* **1931**, *127*, 741.
[2] S. S. Kistler, *J. Phys. Chem.* **1932**, *36*, 52.
[3] J. Innerlohinger,H. K. Weber,G. Kraft, *Macromol. Symp.* **2006**, *244*, 126.
[4] R. Gavillon,PhD Thesis "Preparation et characterization de materiaux cellulosiques ultra poreux", Ecole des Mines de Paris, Ecole Doctorale 364: Sciences Fondamentales et Appliquées, 2006.
[5] J. Gensrich,H.-P. Fink,J. Kunze,E. Schaaf, *Zellcheming Conf. Baden-Baden*, 25th–26th June **2002**, *electronic proceedings in ipw - Das Papier 5* **2003**.
[6] K. Ekman,V. Eklund,J. Fors,J. I. Huttunen,J.-F. Selin,O. T. Turunen, Cellulose Carbamate, in Cellulose-Structure, Modification and Hydrolysis, R. A. Young,R. M. Rowell,Eds., J. Wiley & Sons, New York 1986.
[7] M. Voges,M. Brück,H.-P. Fink,J. Gensrich,Proc. of the Akzo-Nobel Cellulosic Man-made Fiber Seminar **2000**, Stenungsund, Sweden.
[8] U. Prüße,F. Bruske,J. Breford,K.-D. Vorlop, *Chem. Eng. Technol.* **1998**, *21*(2), 153.
[9] E. Lack,H. Seidlitz,M. Sova,F. Lang jr.,V. International Symposium on High Pressure Process Technology and Chemical Engineering, 24th-27th June **2007**, Segovia, Spain.
[10] E. Guilminot,F. Fischer,M. Chatenet,A. Rigacci,S. Berthon-Fabry,P. Achard,E. Chainet, *J. Power Sources* 2007, *166*(1), 104.

[11] D. Gao,Diss. **2003**, TU Freiberg, Germany.
[12] E. W. Washborn, *Proc. Natl. Acad. Sci.* **1921**, *7*, 115.
[13] S. Brunner,P. H. Emmet,E. Teller, *J. Amer. Chem. Soc.* **1938**, *60*, 309.
[14] E. P. Barrett,L. G. Joyner,J. Halenda, *Amer. Chem. Soc.* **1951**, *73*, 373.
[15] G. Horvath,K. Kawazoe, *J. Chem. Eng. Jap.* **1983**, *16, 6*, 470.
[16] H.-P. Fink,E. Walenta, *Das Papier* **1994**, *48*, 739.
[17] O. Kratky,G. Porod, *J. Colloid Sci.* **1949**, *4*, 35;G. Porod, *Kolloid-Z.* **1951**, *124*, 83; **1952**, *125*, 51.